







RESEARCH ARTICLE | AUGUST 14 2023

Magneto-optical imaging of magnetic-domain pinning induced by chiral molecules

Special Collection: [Chiral Induced Spin Selectivity](#)

Yael Kapon ; Fabian Kammerbauer ; Shira Yochelis ; Mathias Kläui ; Yossi Paltiel  

 Check for updates

J. Chem. Phys. 159, 064701 (2023)

<https://doi.org/10.1063/5.0159351>



View
Online



Export
Citation

CrossMark

Magneto-optical imaging of magnetic-domain pinning induced by chiral molecules

Cite as: J. Chem. Phys. 159, 064701 (2023); doi: 10.1063/5.0159351

Submitted: 23 May 2023 • Accepted: 12 July 2023 •

Published Online: 14 August 2023



View Online



Export Citation



CrossMark

Yael Kapon,¹  Fabian Kammerbauer,²  Shira Yochelis,¹  Mathias Kläui,²  and Yossi Paltiel^{1,a)} 

AFFILIATIONS

¹Institute of Applied Physics, Faculty of Sciences, The Hebrew University of Jerusalem, Jerusalem 9190401, Israel

²Institute of Physics, Johannes Gutenberg University Mainz, Staudingerweg 7, 55128 Mainz, Germany

Note: This paper is part of the JCP Special Topic on Chiral Induced Spin Selectivity.

a) Author to whom correspondence should be addressed: paltiel@mail.huji.ac.il

ABSTRACT

Chiral molecules have the potential for creating new magnetic devices by locally manipulating the magnetic properties of metallic surfaces. When chiral polypeptides chemisorb onto ferromagnets, they can induce magnetization locally by spin exchange interactions. However, direct imaging of surface magnetization changes induced by chiral molecules was not previously realized. Here, we use magneto-optical Kerr microscopy to image domains in thin films and show that chiral polypeptides strongly pin domains, increasing the coercive field locally. In our study, we also observe a rotation of the easy magnetic axis toward the out-of-plane, depending on the sample's domain size and the adsorption area. These findings show the potential of chiral molecules to control and manipulate magnetization and open new avenues for future research on the relationship between chirality and magnetization.

Published under an exclusive license by AIP Publishing. <https://doi.org/10.1063/5.0159351>

INTRODUCTION

Over the last thirty years, there has been growing interest in the spin-selective properties of chiral organic materials.¹ When an electron passes through a chiral molecule, it exhibits a preferred spin polarization corresponding to the molecular chirality; this phenomenon is known as the Chirality Induced Spin Selectivity (CISS).^{2,3}

Since its discovery, the CISS effect has shown great promise for applications in spintronics⁴ and enantioselective chemistry.^{1,5} For both lines of study, the interface between chiral molecules and ferromagnets was studied extensively. Two complementary effects have been utilized for this purpose. The first is the enantioselective adsorption of chiral polypeptides on perpendicularly magnetized samples.^{6–12} The second is surface magnetization induced by chiral molecular adsorption,^{13–16} where the chemisorption of L(D)- α helix polyalanine (AHPA) resulted in local magnetization in the up (down) direction perpendicular to the plane without external stimuli, such as light or electric field. Both effects were attributed to thermally induced spin-exchange interactions with the surface.

Furthermore, it was found that there is a correlation between the magnetic easy axis and the tilt angle of the molecule.^{17,18}

The magnetization induced by chiral polypeptides was imaged before using magnetic force microscopy (MFM) imaging,¹³ measuring the magnetic stray field. Sharma *et al.*¹⁹ showed the magnetization switching of the Co thin layer induced by chiral polypeptides using magneto-optical imaging and spectroscopy. While this method measures the magnetization directly, the local flipping of domains in the vicinity of chiral polypeptides has yet to be imaged.

Here, we used Magneto-Optical Kerr Effect (MOKE) microscopy to directly image the impact of chiral polypeptides on the magnetic properties in a sample with sizable perpendicular magnetic anisotropy (PMA) and a sample with in-plane aligned magnetic domains.

MOKE microscopy is a non-invasive imaging method that enables direct imaging of surface magnetization with high spatial resolution.²⁰ This makes it especially interesting to CISS-related research, enabling measurements of the chirality-induced magnetization in a direct and fast way. Kerr microscopy is based on the

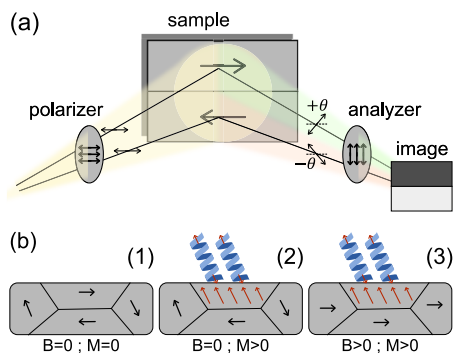


FIG. 1. Magnetization of domains by chiral polypeptides. (a) Magneto-Optical Kerr effect (MOKE) microscopy is used to image the effects of chiral polypeptides on magnetic materials. Linearly polarized light, upon reflection from the surface, rotates in different angles due to different directions of magnetization. The different rotations result in different contrasts in the image plane, allowing for domain imaging. (b) 1—In the absence of an external magnetic field, a demagnetized material lacks a preferential magnetization direction in its domains. 2—However, the adsorption of chiral polypeptides on the surface magnetizes and aligns the domains near them. 3—Upon applying a magnetic field, the domains align with the field except those near the chiral polypeptides. The polypeptide manipulates the magnetic domains in its vicinity.

magneto-optical Kerr effect, which occurs when polarized light is reflected off a magnetized surface. The reflected light undergoes a rotation in polarization due to the interaction between the magnetic moment of the surface and the electric field of the incident light. Different magnetization directions on the surface result in different magnitudes of polarization rotation, which leads to contrast differences in the MOKE microscopy image [see Fig. 1(a)]. This enables direct imaging of magnetic domains and provides valuable insights into the magnetic properties of the sample.

Figure 1(b) presents a sketch of the magnetization changes induced by chiral polypeptides and the domain switching induced by chiral molecule adsorption. The local domain switching can be imaged by MOKE microscopy [Fig. 1(b)]. A non-magnetized magnetic material will have domains magnetized in all directions with zero net magnetization [Fig. 1(b) right]. When chiral peptides adsorb on the surface of the ferromagnet, the domains in the vicinity of the chiral molecule are found to align toward the molecular axis of the molecules [Fig. 1(b-2)]. Following the molecule adsorption, a magnetic field can be applied, aligning the magnetic domains with the field, except the ones in the vicinity of the chiral polypeptides, which will be pinned by the polypeptides [Fig. 1(b-3)]. This will appear as a changed contrast in the MOKE microscope's image.

RESULTS

To directly image the magnetization induced by chiral polypeptides, we used a commercial Evico-Magnetics GmbH, room temperature, Magneto-optical Kerr effect (MOKE) microscope, equipped with electromagnets in a direction perpendicular and parallel to the sample surface. To enhance the magnetic signal contrast, the sample was saturated using a 2 mT out-of-plane magnetic field, and the saturated image was subtracted from the optical image. Reduced noise

was achieved by utilizing active piezo-electric stabilization during the measurement.

It is important to note that the contrast obtained by the MOKE microscope is a qualitative description of the magnetization rather than a quantitative one. The contrast corresponds to a rotation of polarization relative to the analyzer and represents areas of different directions of magnetization relative to the incident plane of light. In the polar mode, we imaged domains perpendicular to the surface plane, while in the longitudinal mode, we imaged in-plane magnetized domains.

Ta(5)/CoFeB(0.9)/MgO(2)/Ta(2)/Au(5 nm) thin films with a significant perpendicular magnetic anisotropy (PMA) were prepared using magnon sputtering using a Singulus Rotaris sputter deposition tool. The samples were intentionally designed to enable easy imaging of domains in the MOKE polar configuration at room temperature; a detailed description can be found in the supplementary material. Magnetization loops are presented in Fig. 2(a). To introduce optically detectable molecular aggregates to the surface, an L- α helix polyalanine (L-AHPA) solution was drop-casted onto the sample and allowed to dry, forming visible aggregates as illustrated by blue arrows in Fig. 2(b), top. As a reference, a-chiral 11-mercapto undecanoic acid aggregates were prepared in the same way. A detailed description of the drop-casting method can also be found in the supplementary material. Subsequently, the domains in the proximity of the chiral aggregates, indicated by orange arrows in the bottom panel of Fig. 2(b), were imaged.

Figure 2(a) displays the magnetization induced by chiral polypeptides. The domains of Ta/CoFeB/MgO/Ta/Au thin films were imaged while sweeping the magnetic field direction from -2 to $+2$ mT. The Kerr intensity was averaged over selected areas (red/black squares). This averaged intensity corresponds to the surface magnetization, which is normalized relative to the saturated intensity. Magnetization loops for Ta/CoFeB/MgO/Ta/Au thin films were measured around the L- α helix polyalanine aggregation (red area) and at a distance from the aggregation (black area) in a polar configuration. A clear change in the magnetization loops was observed near (red) and away from (black) the aggregation.

Since the coercive field of the continuous film of the untreated samples is around 0.1 mT, most domains of the sample flip and align with the field direction as visible by the contrast change to dark when the field is swept from negative to positive and passes a value of 0.1 mT. This expected behavior is not seen for the domains near the aggregation, which remain with bright contrast. It takes another 1 mT to flip all the domains close to the aggregation. Reversing the field direction, sweeping positive to negative, results in the opposite effect. At -0.1 mT, most domains flip to become bright, but it takes another 1 mT in the negative direction to flip the domains close to the aggregation. The effect of the chiral polypeptides is observable in different areas close to the aggregation and is reproducible. Video S1 of the Supplementary material shows an example of flipping as the field is swept from negative to positive and back. This indicates that the adsorbed layer has drastically impacted the anisotropy of the magnetic layer.

The chiral polypeptides increase the coercive field of the chosen PMA sample by 1 mT, which is ten times the original value. Figure S1 of the Supplementary material presents the same

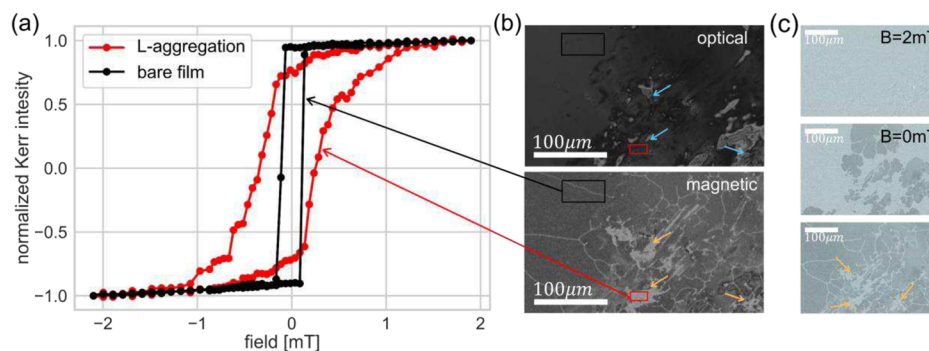


FIG. 2. Magnetization induced by chiral polypeptides. (a) Magnetization hysteresis loops were measured for Ta/CoFeB/MgO/Ta/Au thin films around the aggregation of L- α helix polyalanine (red) and at a distance from the aggregation (black) in a polar configuration. The chiral polypeptides increased the coercive field of the sample by 1 mT, which is ten times the original value. (b) Top: an optical image of the chiral aggregates (blue arrows). Bottom: a MOKE image of the domains held by the chiral aggregation (orange arrows). The scale bar is 100 μm . (c) Demonstration of domain spreading from the chiral polypeptides. At 2 mT, the magnetization is uniformly oriented. When the field is turned off, the magnetization changes and oppositely magnetized domains appear. At a steady state, domains are fixed by the chiral aggregates. The scale bar is 100 μm .

experiment with *a*-chiral aggregates where no change in the magnetic properties of the film was recorded, indicating that the change is derived from the chirality and not from any mechanical or chemical changes to the surface. In addition, the solvent itself does not change the magnetic properties of the magnetic layer as seen in Fig. S2 of the supplementary material. Previous studies¹³ have reported chirality-induced magnetization using magnetic force microscopy (MFM); however, direct imaging of the surface magnetization itself had not been achieved before. It is worth noting that the shape of the magnetization loop changes as well, attributed to the sample area chosen and the extent of flipping. The closer the domains are to the aggregation, the magnetization changes more abruptly. In addition, the oxide layer in the chosen PMA sample likely screens the effect of the chiral polypeptides, and metallic thin films without oxidation may present a stronger effect.

To investigate the effect of the chiral polypeptides in a thermally active dynamic regime, we first saturated the magnetic sample and then turned off the magnetic field to record the domain flipping in real-time, as shown in video S2 of the supplementary material. The corresponding images from the video are displayed in Fig. 2(c). At 2 mT, the magnetization is uniform, and the domains appear bright [Fig. 2(c), top]. When the magnetic field is turned off, the magnetization flips and dark domains emerge [Fig. 2(c), middle]. The dark domains spread from the chiral aggregates, indicating that the chiral aggregates act as pinning sites. In a steady state, the chiral aggregates pin the light domains in place, as indicated by the orange arrows in Fig. 2(c), bottom. This observation corroborates the effect seen in the magnetization hysteresis loops. In the *a*-chiral case, no correlation was seen between the domain flipping and aggregates, as presented in Fig. S1.

The induced changes of the magnetization were observed perpendicular to the plane and using aggregates that do not have a specific orientation compared to the sample. Previous papers have also shown a correspondence between the magnetic easy axis and monolayer tilt angle.^{17,18} These studies characterized the magnetic easy

axis fully by vectorial magnetic field measurements while measuring the monolayer tilt angle using atomic force microscopy and found a correlation between the two. To observe the correlation, a sample with in-plane domains with a monolayer adsorption was imaged. A sample of Ti(2)/Ni(80)/Au(5 nm) was prepared by magnon sputtering as described in the supplementary material. The resulting sample had in-plane domains that were imaged in the longitudinal mode. The sample was prepared in such a way that the averaged domain size was on a 50 μm scale, large enough to be imaged optically (in the longitudinal configuration).

On the Ni sample, we adsorbed a monolayer of L-AHPA using a self-assembly process, discussed further in the section titled “Methods.” Previous studies found such monolayers have a uniform tilt angle of 30°–60° normal to the surface^{18,21} due to their self-assembling properties, and so it is well-suited for exploring the effects of the molecular axis vs the magnetic easy axis. By utilizing electron beam lithography, we were able to selectively adsorb polypeptides onto different rectangular areas with widths starting from 5 to 60 μm , resulting in varying sizes of adsorption regions that enable to probe different local effects.

Figure 3 shows magnetization loops in the longitudinal configuration of L-AHPA adsorbed on Ti(2)/Ni(80)/Au(5) samples of various monolayer sizes (ranging from 5 \times 300 to 60 \times 1000 μm^2). The remanent magnetization (the magnetization at zero field) for the largest monolayer area (red) is smaller than that of the bare magnetic sample (purple), indicating a rotation of the easy axis from the in-plane toward the out-of-plane. The tilt of the easy axis depends on the monolayer area, with the hysteresis loop softening as the monolayer size increases, reaching saturation above 20 \times 600 μm^2 adsorption area, which matches the sample’s domain size (50 \times 10 μm^2). The rotation of the easy axis is connected to the CISS effect due to the correlation between the tilt angle of the monolayer’s molecular axis compared to the surface, as sketched in Fig. 3(b).

To test the importance of domain size compared to the adsorption area, two samples with different domain sizes were used. Thus,

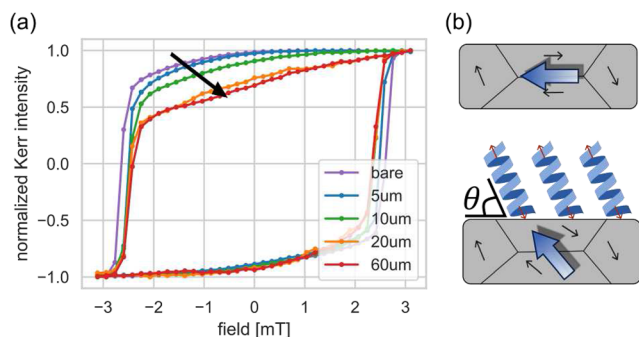


FIG. 3. Rotation of the easy magnetic axis by a chiral monolayer in an in-plane ferromagnet. (a) In-plane magneto-optical magnetization loop for a Ti(2 nm)/Ni(80 nm)/Au(5 nm) sample (purple) with L- α helix polyaniline adsorbed on different areas: $60 \times 1000 \mu\text{m}^2$ (red), $20 \times 600 \mu\text{m}^2$ (orange), $10 \times 300 \mu\text{m}^2$ (green), and $5 \times 300 \mu\text{m}^2$ (blue). As the adsorption area increases, the remanent magnetization for the in-plane contrast measurement decreases, indicating a rotation of the easy axis toward the out-of-plane direction. (b) Illustration of the rotation of the magnetic easy axis (blue). After monolayer adsorption, the magnetic easy axis couples with the molecular tilt angle (θ).

the remanent magnetization in the MOKE magnetization loops on samples of Ti(2 nm)/Ni(30/80 nm)/Au(5 nm) sputtered and patterned with a chiral L-AHPA monolayer by a self-assembly process was measured. Figure 4(a) shows the remanent magnetization of the sample decrease with adsorption area, with both 8/80/5 nm (red) and 8/30/5 nm (blue) samples showing a decrease, but with a smaller effect in the latter. The asymmetry in the hysteresis loops was considered by averaging the remanent magnetization on the sweep up and down. When a full monolayer, much bigger than the domains sizes, was adsorbed on the surface, the remanent magnetization is closer to the unperturbed sample. In that case, remanent magnetization of the full monolayer is similar for the two thicknesses. Therefore, the monolayer and domain sizes have to match

to achieve the strongest changes in magnetic properties. The different Ni thickness translates to different average domain sizes, as seen in Fig. 4(b). While the 80 nm Ni thickness has smaller domains ($50 \mu\text{m}$), the 30 nm Ni domains are larger, above the optical field of view of the microscope ($>500 \mu\text{m}$). Therefore, the results point to the importance of domain size as compared to the adsorption area. There is an expected match between the domain size and adsorption area.

Finally, to connect all the above results to the molecular chirality in opposition to surface effects induced by adsorption or treatment prior to adsorption, we tested the magnetization loops of Ti(2 nm)/Ni(30)/Au(5 nm) (orange) with a patterned monolayer of L-AHPA (purple) (size was $60 \times 1000 \mu\text{m}^2$) D-AHPA (red) and a-chiral mercaptoundecanoic acid (green) (size was $60 \times 700 \mu\text{m}^2$). The rotation of the easy-axis was observed similarly between L and D chirality, while a-chiral mercaptoundecanoic acid adsorption had only a small effect. This indicates the changes in magneto-optical properties observed in this paper were a result of the chiral molecule-induced manipulation of the magnetic properties.

DISCUSSION

In this study, we presented a direct spatial imaging of chiral-molecule-induced enhanced coercivity (pinning) of magnetization due to manipulation of the anisotropy. Our results demonstrate that chiral aggregates cause a drastic increase in the coercive field of 1 mT in a perpendicular magnetization of thin films. This change in magnetic properties is accompanied by the strong pinning of domains to the chiral aggregates, as revealed by domain imaging. In addition, real-time measured domain flipping originating from the chiral aggregates was observed, suggesting that there is an interacting force that is stable after adsorption between the magnetic domains and the chiral molecules. Different mechanisms can lead to such behavior. In general, the observed changes of the magnetic switching imply a strongly changed effective anisotropy. We relate this to a possible interaction between thermally induced spin polarization^{15,22,23}

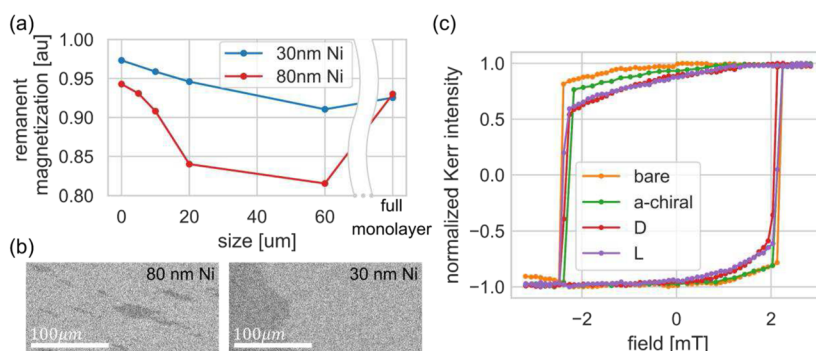


FIG. 4. Effect of L- α helix polyaniline adsorption on magneto-optical effects of Ti(2 nm)/Ni(30/80 nm)/Au(5 nm) samples. (a) The remanent magnetization of the sample decreases with adsorption area, with both 8/80/5 nm (red) and 8/30/5 nm (blue) samples showing a decrease, but with a smaller effect in the latter due to its larger domain size. When adsorption area is much larger than average domains size, the remanent magnetization increases and is the same for both samples. (b) Magnetic imaging shows smaller domains for 80 nm Ni ($50 \times 10 \mu\text{m}^2$) than 30 nm Ni ($>500 \times 500 \mu\text{m}^2$). (c) Magnetization loops of L- (purple) and D- (red) α helix polyaniline adsorption show a rotation of the easy axis (adsorption size is $60 \times 700 \mu\text{m}^2$), while a-chiral mercaptoundecanoic acid (green) adsorption has only a small effect compared with the Ti(2)/Ni(30)/Au(5) sample (orange). The scale bar is $100 \mu\text{m}$.

and the spins of the magnetic layer. Several theoretical papers^{11,24,25} and experimental observations^{13,26–29} suggest the induced change in magnetic properties is derived from spin-exchange interactions between the chiral polypeptides and the sample. Unlike previous studies,¹³ no exchange bias is observed; this may be a result orientation locking between the molecules and the surface magnetization and the large thickness of the samples that reduce the effect of the surface.

While magnetization induced by chiral polypeptides had been previously observed using MFM,¹³ this study has achieved direct imaging of surface magnetization. The interplay between the molecular tilt angle and magnetic easy axis, which was previously explored,^{17,18} was confirmed indicatively through direct imaging of the domains in the vicinity of the chiral monolayer. The magnetic effects observed in this study are interfacial effects imaged in the surface between the chiral polypeptides and the magnetic layer. The main observation in this work may also be relevant to the origin of homochirality in life, as suggested by the avalanche mechanism presented in by Ozturk *et al.*³⁰

Samples with observable domains in the longitudinal configuration and in-plane easy axis were fabricated to observe the effects parallel to the surface. In these samples, a direct coupling between the molecular alignment axis of the chiral monolayer and the magnetic easy axis was measured, as evidenced by a decrease in the remanent magnetization of the magnetic layer after the chiral monolayer's adsorption. We also investigated the connection between the domain size and monolayer area and found that the maximum effect is achieved when there is a matching between the two. A reference sample showed that while L and D AHPA reduced the remanent magnetization of the magnetic layer, the *a*-chiral monolayer had little effect on the magnetic properties.

As demonstrated in this study, MOKE microscopy and MOKE magnetometry offer promising avenues for observing and studying induced pinning effects by chiral molecules. The ability to directly observe surface magnetization is particularly important in CISS-related studies, where the effects are strongest at the interface. The magnetization effect observed in our study has the potential to be scaled down to a sample with smaller domains and adsorption areas, as demonstrated in previous work, using different imaging methods.¹³ It is important to note that the change in coercivity leading to domain-pinning observed in our study is a local and permanent change in magnetic properties and will change the dynamic behavior. An interesting approach would be to observe the domains in real-time during the adsorption process to directly observe the magnetization induced by the adsorption itself, which, however, goes beyond the scope of the current work.

Another avenue of research that could be explored using the same measurement concepts demonstrated in this study is the temperature dependence of the chirality-induced magnetization effect. Both the CISS effect and magnetization of ferromagnets are known to be temperature-dependent,^{15,22} and studying the effect of temperature on these measurements would provide valuable insights into the underlying mechanisms of the effect. These studies would further our understanding of the complex interplay between chirality and magnetism, with potential implications for the development of new technologies.

CONCLUSIONS

In this study, we used MOKE microscopy to directly image the changes in the magnetic properties leading to strong pinning of domains in ferromagnetic perpendicular magnetic anisotropy thin films by chiral polypeptides. In addition, tilting of the magnetic easy magnetization axis was observed toward the molecule alignment axis of an adsorbed molecular monolayer. This non-invasive imaging method allowed us to observe the local magnetization and magnetic effects at the interface between the chiral polypeptides and magnetic samples. Our results show that magnetic domains are affected even outside the adsorption area, while a maximum effect is achieved when the domain size matches the adsorption area. Our findings offer new perspectives for the study of the CISS effect and its potential applications in the future.

SUPPLEMENTARY MATERIAL

The supplementary material contains video S1 (magnetization flipping during magnetization loops), video S2 (magnetization flipping when turning off the magnetic field), methods and materials, figure S1 (magnetization loops of *a*-chiral aggregation), and figure S2 (magnetization loops of ethanol solution vs bare substrate).

ACKNOWLEDGMENTS:

The authors are grateful to the Zeiss Foundation HYMMMS project and the Deutsche Forschungsgemeinschaft (DFG, German Research Foundation) [Grant No. 403502522-SPP 2137 Skyrmionics, SFB TRR 173 Spin + X (Project Nos. A01 #268565370 and B02 #268565370)]. M.K. acknowledges the support from the European Union's Horizon 2020 research and innovation program under Grant No. 856538 (3D MAGIC) and the TopDyn Center for Dynamics and Topology. Y.P. acknowledges the support of the BSF (Grant No. 2022503), Horizon EU Marie Skłodowska Curie (DN) CISSE grant, and The Ministry of Innovation, Science and Technology (Grant No. 7500157).

AUTHOR DECLARATIONS

Conflict of Interest

The authors have no conflicts to disclose.

Author Contributions

Yael Kapon: Conceptualization (equal); Investigation (equal); Writing – original draft (equal); Writing – review & editing (equal). **Fabian Kammerbauer:** Resources (equal); Writing – review & editing (equal). **Shira Yochelis:** Supervision (equal); Writing – review & editing (equal). **Mathias Klau:** Resources (equal); Supervision (equal); Writing – review & editing (equal). **Yossi Paltiel:** Conceptualization (equal); Supervision (equal); Writing – review & editing (equal).

DATA AVAILABILITY

The data that support the findings of this study are available from the corresponding author upon reasonable request.

REFERENCES

- ¹R. Naaman, Y. Paltiel, and D. H. Waldeck, "Chiral molecules and the electron spin," *Nat. Rev. Chem.* **3**(4), 250–260 (2019).
- ²K. Ray, S. P. Ananthavel, D. H. Waldeck, and R. Naaman, "Asymmetric scattering of polarized electrons by organized organic films of chiral molecules," *Science* **283**(5403), 814–816 (1999).
- ³F. Evers, A. Aharony, N. Bar-Gill, O. Entin-Wohlman, P. Hedegård, O. Hod, P. Jelinek, G. Kamieniarz, M. Lemeshko, K. Michaeli, V. Mujica, R. Naaman, Y. Paltiel, S. Refaely-Abramson, O. Tal, J. Thijssen, M. Thoss, J. M. van Ruitenbeek, L. Venkataraman, D. H. Waldeck, B. Yan, and L. Kronik, "Theory of chirality induced spin selectivity: Progress and challenges," *Adv. Mater.* **34**(13), 2106629 (2022).
- ⁴Z. Shang, T. Liu, Q. Yang, S. Cui, K. Xu, Y. Zhang, J. Deng, T. Zhai, and X. Wang, "Chiral-molecule-based spintronic devices," *Small* **18**(32), 2203015 (2022).
- ⁵R. Naaman, Y. Paltiel, and D. H. Waldeck, "Chiral induced spin selectivity gives a new twist on spin-control in chemistry," *Acc. Chem. Res.* **53**(11), 2659–2667 (2020).
- ⁶K. Banerjee-Ghosh, O. Ben Dor, F. Tassinari, E. Capua, S. Yochelis, A. Capua, S.-H. Yang, S. S. P. Parkin, S. Sarkar, L. Kronik, L. T. Baczewski, R. Naaman, and Y. Paltiel, "Separation of enantiomers by their enantiospecific interaction with achiral magnetic substrates," *Science* **360**(6395), 1331–1334 (2018).
- ⁷F. Tassinari, J. Steidel, S. Paltiel, C. Fontanesi, M. Lahav, Y. Paltiel, and R. Naaman, "Enantioseparation by crystallization using magnetic substrates," *Chem. Sci.* **10**(20), 5246–5250 (2019).
- ⁸Y. Lu, B. P. Bloom, S. Qian, and D. H. Waldeck, "Enantiospecificity of cysteine adsorption on a ferromagnetic surface: Is it kinetically or thermodynamically controlled?," *J. Phys. Chem. Lett.* **12**(32), 7854–7858 (2021).
- ⁹S. F. Ozturk and D. D. Sasselov, "On the origins of life's homochirality: Inducing enantiomeric excess with spin-polarized electrons," *Proc. Natl. Acad. Sci. U. S. A.* **119**(28), e2204765119 (2022).
- ¹⁰M. R. Safari, F. Matthes, K.-H. Ernst, D. E. Bürgler, and C. M. Schneider, "Enantiospecific adsorption on a ferromagnetic surface at the single-molecule scale," [arXiv:2211.12976](https://arxiv.org/abs/2211.12976) (2022).
- ¹¹A. Dianat, R. Gutierrez, H. Alpern, V. Mujica, A. Ziv, S. Yochelis, O. Millo, Y. Paltiel, and G. Cuniberti, "Role of exchange interactions in the magnetic response and intermolecular recognition of chiral molecules," *Nano Lett.* **20**(10), 7077–7086 (2020).
- ¹²J. Fransson, "Charge and spin dynamics and enantioselectivity in chiral molecules," *J. Phys. Chem. Lett.* **13**(3), 808–814 (2022).
- ¹³O. Ben Dor, S. Yochelis, A. Radko, K. Vankayala, E. Capua, A. Capua, S.-H. Yang, L. T. Baczewski, S. S. P. Parkin, R. Naaman, and Y. Paltiel, "Magnetization switching in ferromagnets by adsorbed chiral molecules without current or external magnetic field," *Nat. Commun.* **8**(1), 14567 (2017).
- ¹⁴S. Dalum and P. Hedegård, "Theory of chiral induced spin selectivity," *Nano Lett.* **19**(8), 5253–5259 (2019).
- ¹⁵J. Fransson, "Vibrational origin of exchange splitting and chiral-induced spin selectivity," *Phys. Rev. B* **102**(23), 235416 (2020).
- ¹⁶S. Alwan and Y. Dubi, "Spinterface origin for the chirality-induced spin-selectivity effect," *J. Am. Chem. Soc.* **143**(35), 14235–14241 (2021).
- ¹⁷I. Meirzada, N. Sukenik, G. Haim, S. Yochelis, L. T. Baczewski, Y. Paltiel, and N. Bar-Gill, "Long-time-scale magnetization ordering induced by an adsorbed chiral monolayer on ferromagnets," *ACS Nano* **15**(3), 5574–5579 (2021).
- ¹⁸N. Sukenik, F. Tassinari, S. Yochelis, O. Millo, L. T. Baczewski, and Y. Paltiel, "Correlation between ferromagnetic layer easy axis and the tilt angle of self assembled chiral molecules," *Molecules* **25**(24), 6036 (2020).
- ¹⁹A. Sharma, P. Matthes, I. Soldatov, S. S. P. K. Arekapudi, B. Böhm, M. Lindner, O. Selyshchev, N. Thi Ngoc Ha, M. Mehring, C. Tegenkamp, S. E. Schulz, D. R. T. Zahn, Y. Paltiel, O. Hellwig, and G. Salvan, "Control of magneto-optical properties of cobalt-layers by adsorption of α -helical polyalanine self-assembled monolayers," *J. Mater. Chem. C* **8**(34), 11822–11829 (2020).
- ²⁰A. Hubert and R. Schäfer, *Magnetic Domains: Analysis of Magnetic Microstructures* (Springer, Berlin, Heidelberg, 1998), pp. 11–97.
- ²¹Y. Miura, S. Kimura, Y. Imanishi, and J. Umemura, "Formation of oriented helical peptide layers on a gold surface due to the self-assembling properties of peptides," *Langmuir* **14**(24), 6935–6940 (1998).
- ²²T. K. Das, F. Tassinari, R. Naaman, and J. Fransson, "Temperature-dependent chiral-induced spin selectivity effect: Experiments and theory," *J. Phys. Chem. C* **126**(6), 3257–3264 (2022).
- ²³K. Kondou, M. Shiga, S. Sakamoto, H. Inuzuka, A. Nihonyanagi, F. Araoka, M. Kobayashi, S. Miwa, D. Miyajima, and Y. Otani, "Chirality-induced magnetoresistance due to thermally driven spin polarization," *J. Am. Chem. Soc.* **144**(16), 7302–7307 (2022).
- ²⁴J. Fransson, "Charge redistribution and spin polarization driven by correlation induced electron exchange in chiral molecules," *Nano Lett.* **21**(7), 3026–3032 (2021).
- ²⁵S. Naskar, V. Mujica, and C. Herrmann, "Chiral-induced spin selectivity and non-equilibrium spin accumulation in molecules and interfaces: A first-principles study," *J. Phys. Chem. Lett.* **14**(3), 694–701 (2023).
- ²⁶A. Ziv, A. Saha, H. Alpern, N. Sukenik, L. T. Baczewski, S. Yochelis, M. Reches, and Y. Paltiel, "AFM-based spin-exchange microscopy using chiral molecules," *Adv. Mater.* **31**(40), 1904206 (2019).
- ²⁷E. Z. B. Smolinsky, A. Neubauer, A. Kumar, S. Yochelis, E. Capua, R. Carmieli, Y. Paltiel, R. Naaman, and K. Michaeli, "Electric field-controlled magnetization in GaAs/AlGaAs heterostructures–chiral organic molecules hybrids," *J. Phys. Chem. Lett.* **10**(5), 1139–1145 (2019).
- ²⁸S. Ghosh, S. Mishra, E. Avigad, B. P. Bloom, L. T. Baczewski, S. Yochelis, Y. Paltiel, R. Naaman, and D. H. Waldeck, "Effect of chiral molecules on the electron's spin wavefunction at interfaces," *J. Phys. Chem. Lett.* **11**(4), 1550–1557 (2020).
- ²⁹F. Tassinari, D. Amsallem, B. P. Bloom, Y. Lu, A. Bedi, D. H. Waldeck, O. Gidron, and R. Naaman, "Spin-dependent enantioselective electropolymerization," *J. Phys. Chem. C* **124**(38), 20974–20980 (2020).
- ³⁰S. F. Ozturk, D. K. Bhowmick, Y. Kapon, Y. Sang, A. Kumar, Y. Paltiel, R. Naaman, and D. D. Sasselov, "Chirality-induced magnetization of magnetite by an RNA precursor," [arXiv:2304.09095](https://arxiv.org/abs/2304.09095) (2023).